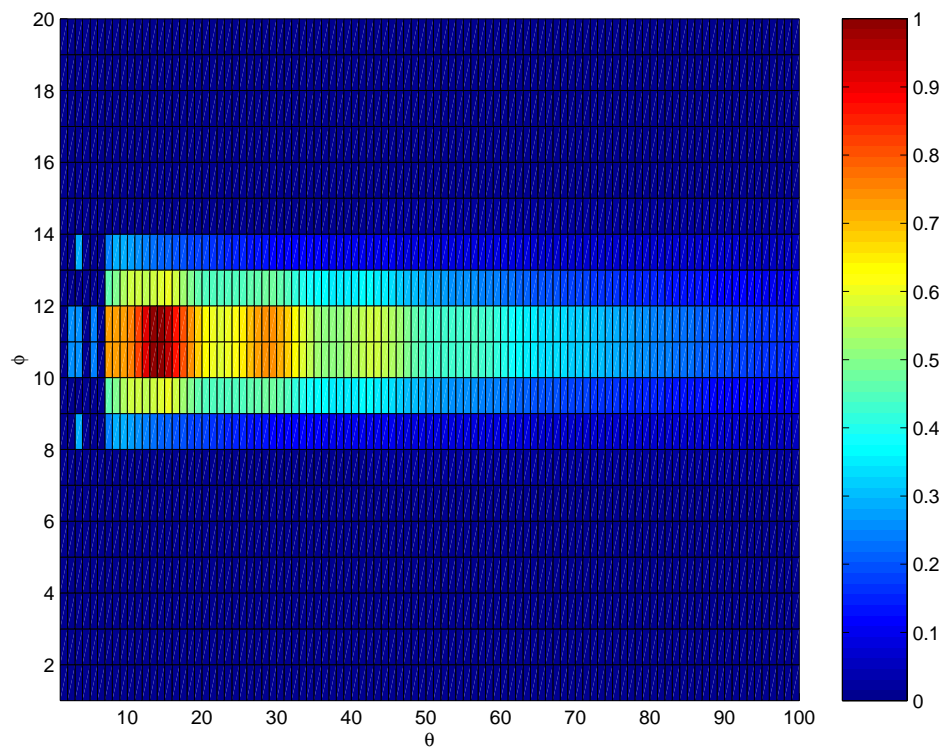


Marlene Andersson

# Validation of the Computer Program SIGGE against Spectral IR-measurements on an Engine Test Rig





Marlene Andersson

# **Validation of the Computer Program SIGGE against Spectral IR-measurements on an Engine Test Rig**



## Abstract

The IR-signature code SIGGE has been validated, using spectral IR-measurements on an engine test rig. Calculations of IR-radiation from gases, such as CO<sub>2</sub> and H<sub>2</sub>O, have been compared with experimental data. The calculations have been made in the wave-number interval  $\eta = 1500 \text{ cm}^{-1} - 4500 \text{ cm}^{-1}$ , with three different resolutions,  $\Delta\eta = 5 \text{ cm}^{-1}$ ,  $16 \text{ cm}^{-1}$  and  $25 \text{ cm}^{-1}$ . The result is satisfactory and further developments of SIGGE will proceed.



# Contents

<b>1</b>	<b>Introduction</b>	<b>7</b>
<b>2</b>	<b>Basic concepts of the program</b>	<b>9</b>
<b>3</b>	<b>A short description of the experiment</b>	<b>13</b>
<b>4</b>	<b>Description of the validation case</b>	<b>15</b>
4.1	CFD-calculation . . . . .	15
4.2	Definition of validation cases . . . . .	17
<b>5</b>	<b>Results</b>	<b>21</b>
<b>6</b>	<b>Conclusions and outlook</b>	<b>27</b>
	<b>Acknowledgements</b>	<b>29</b>
	<b>References</b>	<b>31</b>





# 1 Introduction

A vehicle will radiate heat in form of infrared (IR) radiation. The intensity of the radiation is dependent on the temperature and the structure of the surface. In a gas, the IR-radiation heat transfer depends on the temperature and the composition of the gas. Different vehicles will emit IR-radiation of different wavelength and intensity, this will give rise to an IR-signature. For an airborne vehicle, the hot plume contributes largely to the IR-signature. For some military vehicle, it is of most importance to have a low IR-signature.

The Department of Computational Aerodynamics, Aeronautics Division (FFA), at the Swedish Defence Research Agency (FOI), is developing a code, SIGGE, for calculating the spectral intensity of IR-radiation [1, 2]. Currently, a  $\beta$ -version of SIGGE exists and as part of the ongoing work, the code has to be validated. This report describes the validation that has been done, where calculations were compared with experimental data.

The parts of SIGGE being validated were the geometric representation using axisymmetry and spectral intensity calculations in a gas containing CO<sub>2</sub> and H<sub>2</sub>O, using different wave-number resolutions. The impact of changes in the input data was also tested.

The experimental data has been acquired from the Department of IR Systems, Sensor Technology, FOI [3]. They have made IR-measurements on an engine test rig, which gave a validation case close to reality.

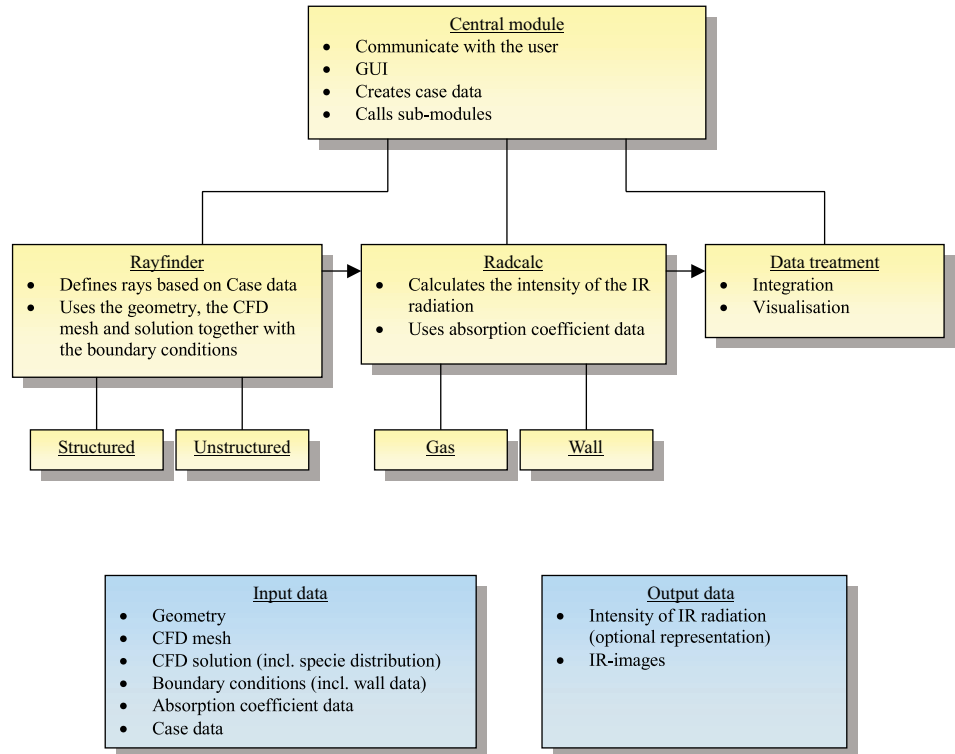
In section 2, a short description of SIGGE is found. In section 3, the experimental measurement is described. The validation case is described in section 4. The results are collected in section 5. Conclusions and outlook are found in section 6.



## 2 Basic concepts of the program

The proposed structure of SIGGE is presented in Figure 1. The code is module

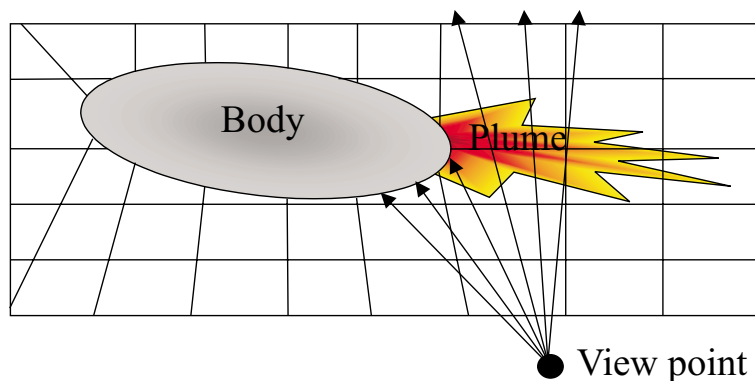
Figure 1. The proposed structure of the module based code SIGGE.



based, where each module can operate alone or together with other modules. In the present version of SIGGE, only the modules RAYFINDER and RADCALC are implemented. Thus, these were the modules tested in this validation.

The program SIGGE uses a CFD-solution<sup>1</sup> as input. The area of interest is divided into small volume units, giving a mesh, see Figure 2. In each volume

Figure 2. Rays are drawn from a view position toward an object in space through a mesh.

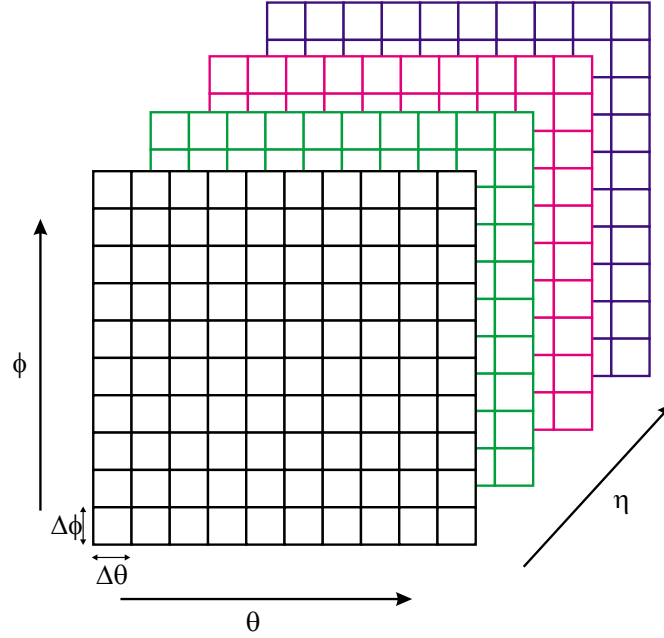


unit the CFD-solution gives a value for variables such as temperature, pressure and mass fraction. The mass fraction is defined as the fraction between ambient air and combustion gas. In the present version of SIGGE, it is assumed that the ambient air will not contain species that will contribute to the IR-signature. The resulting spectra, therefore, have to be corrected for atmospheric moderation.

<sup>1</sup>CFD - Computational Fluid Dynamics

The user will define an imaginary sensor, which consists of a flat plane with a number of pixels, giving an IR-image for each specified wave number, see Figure 3. The orientation of the sensor in space is defined by two orthogonal vectors,

Figure 3. Imaginary sensor defined by the user. The sensor will collect one image for each wave number,  $\eta$ , specified. Each pixel has the field-of-view:  $\Delta\theta \times \Delta\phi$ .



$\hat{\theta}$  and  $\hat{\phi}$ . Each pixel has a field-of-view of  $\Delta\theta \times \Delta\phi$ , which gives a total field-of-view of  $n_\theta\Delta\theta$  and  $n_\phi\Delta\phi$ , where  $n_\theta$  and  $n_\phi$  are the number of pixels in the  $\hat{\theta}$ - and  $\hat{\phi}$ -directions, respectively. The number of rays,  $n_\theta \times n_\phi$ , and the angular resolution,  $\Delta\theta \times \Delta\phi$ , are defined by the user.

The user will also define a view position, which is the position where the imaginary sensor is located, and a target position, which is the position in space where the centre of the sensor is aiming at, giving an aiming direction, which should be orthogonal to the sensor plane.

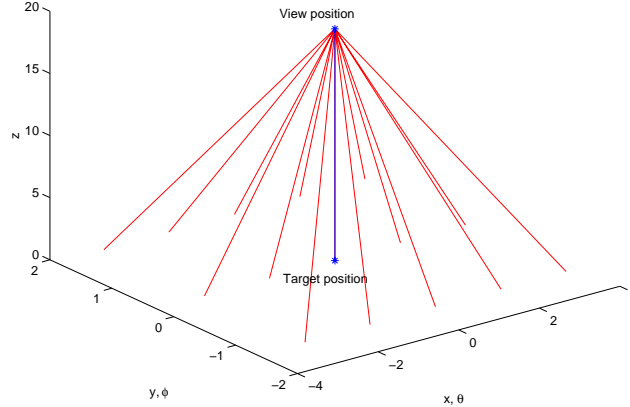
The module RAYFINDER will use this information to draw rays from the view position through the mesh. Each ray will be separated from their neighbours with angles of  $\Delta\theta$  and  $\Delta\phi$ . Thus, each ray will correspond to a pixel in the imaginary sensor. In Figure 4, a view position and a target position are defined in space, making, in this case, the aiming direction of the sensor run along the z-axis. The imaginary sensor will, therefore, coincide with the x-y plane and the  $\hat{\theta}$ -direction can be chosen to run along the x-axis and, consistently, the  $\hat{\phi}$ -direction will run along the y-axis.

If the mesh is axisymmetric, it does not have to cover the whole space, see section 4.1. The module RAYFINDER will mirror the mesh around the axisymmetrical axis and associate the values from the CFD-solution with cells in a virtual mesh.

In the module RADCALC, the spectral intensity,  $I_\eta$ , is calculated for each ray with:

$$\begin{aligned}
 I_\eta(s) = & L_{b\eta}^1 (1 - e^{-\kappa_\eta^1 s_1}) \mathbf{A}_1 + \\
 & + L_{b\eta}^2 e^{-\kappa_\eta^1 s_1} (1 - e^{-\kappa_\eta^2 s_2}) \mathbf{A}_2 + \\
 & + L_{b\eta}^3 e^{-\kappa_\eta^1 s_1} e^{-\kappa_\eta^2 s_2} (1 - e^{-\kappa_\eta^3 s_3}) \mathbf{A}_3 + \dots
 \end{aligned} \tag{1}$$

Figure 4. Rays are drawn from a view position where the centre-ray is drawn toward the target position. Each ray is separated from the neighbouring rays with angles of  $\Delta\theta$  and  $\Delta\phi$ .



where  $\eta$  is the wave number,  $\kappa_\eta$  is the absorption coefficient,  $s_i$  is the length of the specific volume element and  $A_i$  is an area segment defined as:

$$A_i = t_i^2 \Delta\theta \Delta\phi \quad (2)$$

where  $t_i$  is the distance from the view position to the volume element and  $\Delta\theta \times \Delta\phi$  is the angular resolution discussed above.  $L_{b\eta}$  is the spectral black body radiance given by:

$$L_{b\eta} = \frac{2\pi hc_0^2 \eta^3}{\pi(e^{hc_0\eta/kT} - 1)} = \frac{C_1 \eta^3}{e^{C_2\eta/T} - 1} \quad (3)$$

where

$$C_1 = 2hc_0^2 = 1.191 \cdot 10^{-16} Wm^2 \quad (4)$$

$$C_2 = hc_0/k = 1.4388 \cdot 10^{-2} Km \quad (5)$$

These equations are derived in Ref. [1].

The absorption coefficients vary for different species and are dependent on the wave number, the temperature and the distribution of species. The distribution of species can be calculated from the mass fraction, given in the CFD-solution [1]. The absorption coefficients are stored in a data base. The outcome of the calculation is dependent on the quality and correctness of the data base and the CFD-solution.

The user will have to define, among other things, the following variables in an input file:

- View position
- Target position
- Number of rays
- Field-of-view

- Wave-number interval of interest and resolution
- Species
- Input and output files

In this validation, walls and atmospheric background were not taken into consideration.

The result from the IR-calculation is a spectral intensity for each ray. If many rays are used, all spectral intensities of all rays can be summarised giving a total spectral intensity. The space resolution can be represented by an IR-image, where the intensity for each ray is integrated over the wave numbers.

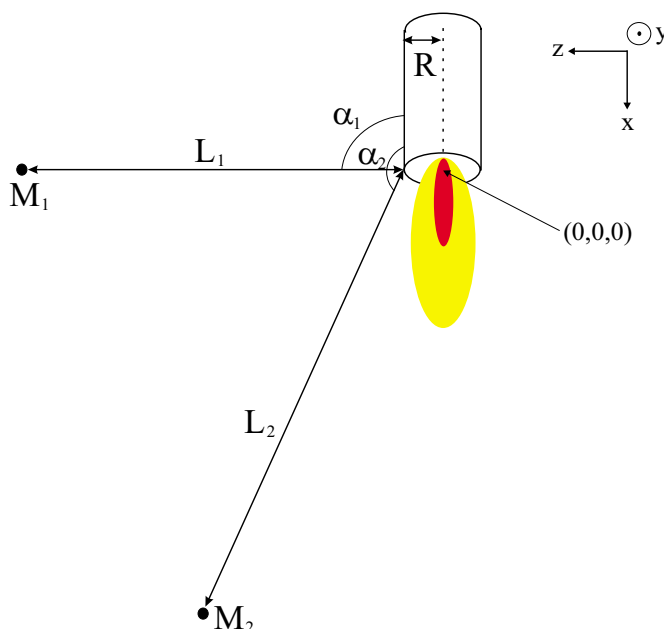
For a more complete description of the theory behind the code and a description of the code itself, see Ref. [1] and Ref. [2].

### 3 A short description of the experiment

The Department of IR Systems, Sensor Technology, FOI, has done spectral IR-measurements on an engine test rig at the Department of Military Engines, at Volvo Aero Corporation (VAC) in Trollhättan, [3]. The engine rig comprises a RM8B-flame pipe, which works as a gas generator, and a combustion zone, where simulated wind speed air is mixed in. At the end a circular nozzle is mounted. The measurements were performed by using the imaging spectrometer, ScanSpec [4, 5].

The simulated free-stream air speed corresponded to a Mach number of approximately 0.6 and the surrounding temperature was around 290 K. The spectrometer was placed at two different measuring positions,  $M_1$  and  $M_2$ , see Figure 5. The distance to the rig was of the same order of magnitude for both position,

Figure 5. A schematic sketch of the experimental set up.



$L_1 \approx L_2 \approx 20$  m, but the angles to the rig differed. Position  $M_1$  corresponded to an angle of  $\alpha_1 = 90^\circ$  and position  $M_2$  to  $\alpha_2 = 162^\circ$ . In the validation, only measuring position  $M_1$  was used. Measuring with ScanSpec, two different wave-number resolutions were used,  $\Delta\eta = 4 \text{ cm}^{-1}$  and  $16 \text{ cm}^{-1}$ . The resolution  $\Delta\eta = 16 \text{ cm}^{-1}$  was required to acquire larger images. Data was acquired for wave numbers between approximately  $1500 \text{ cm}^{-1}$  and  $6000 \text{ cm}^{-1}$ .





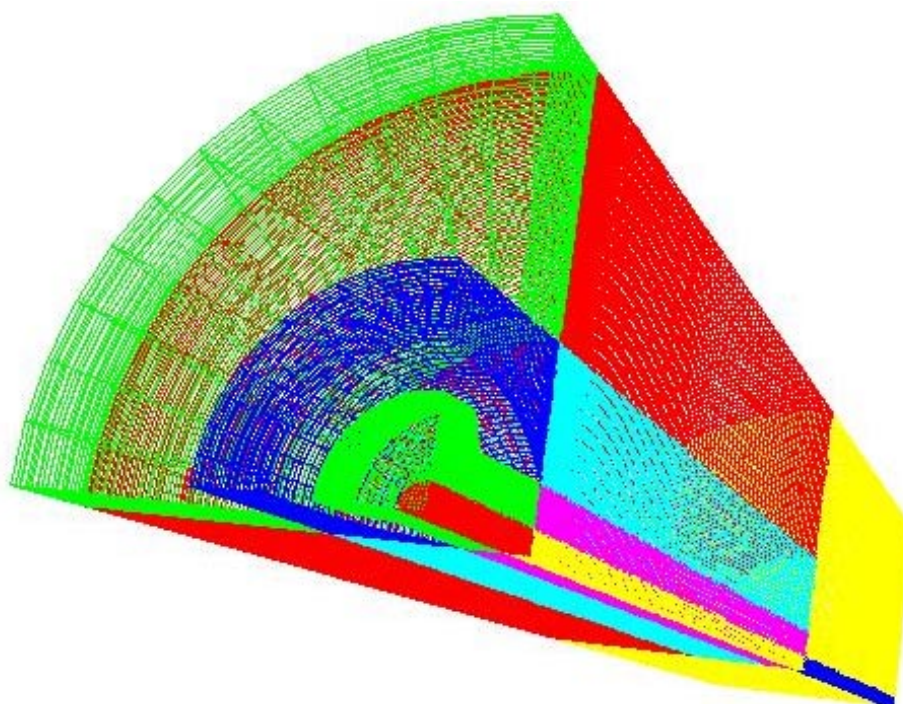
## 4 Description of the validation case

### 4.1 CFD-calculation

The CFD-calculations were made by the Department of Military Engines, VAC, using the solver VOLSOL [6]. The Navier-Stokes equations were solved and the  $k-\varepsilon$  turbulence model was used. The CFD-calculation corresponds to the experiment described in section 3, where the free-stream-values used were temperature  $T = 290.75$  K, pressure  $p = 101000$  Pa and Mach number  $M = 0.6$ .

In Figure 6, the block-structured mesh is presented. The problem is axisym-

Figure 6. One quadrant of the axisymmetrical mesh. The different blocks are represented in different colours.

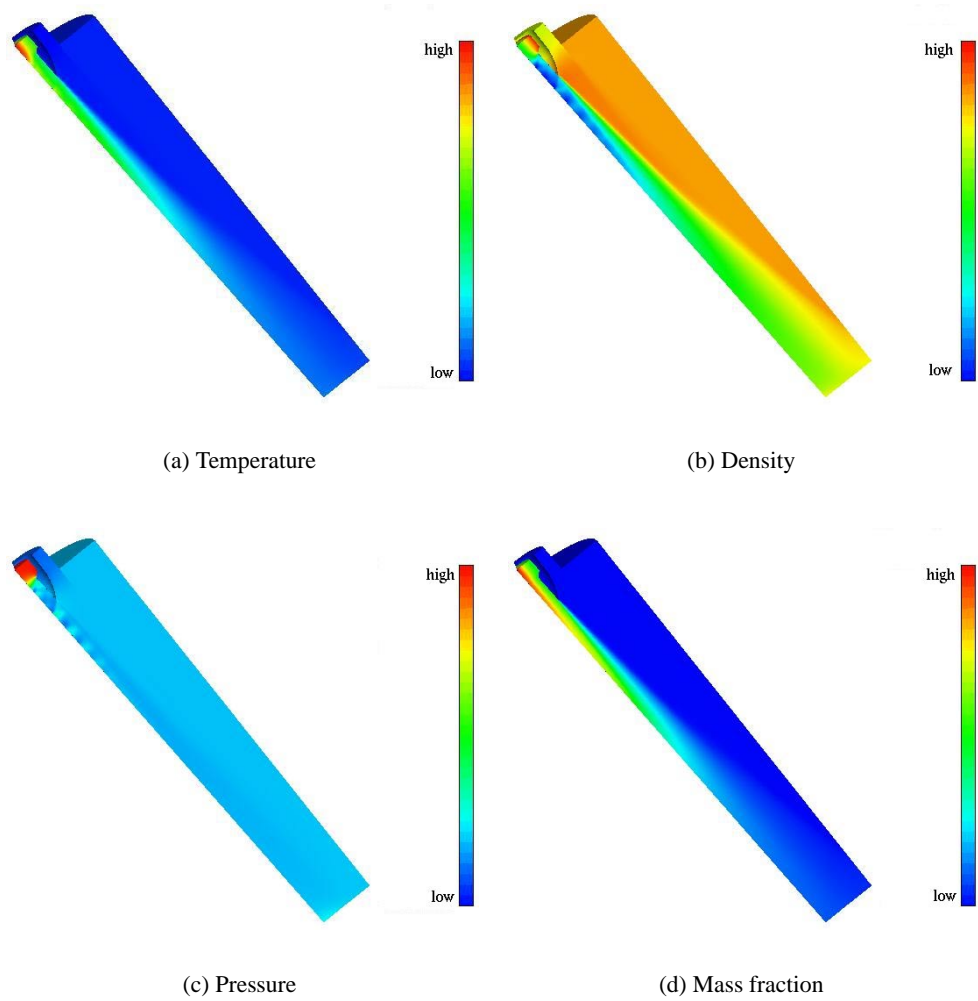


metrical, so only a fourth of the mesh was needed for the calculations. The mesh consists of  $\sim 160000$  cells. It starts with the area around the nozzles and the main part of the mesh represents the volume behind the nozzle.

In Figure 7, some selected variables given in the CFD-solution are presented. The lowest values correspond to the free-stream-values. The maximum temperature is  $T \approx 1000$  K. In the density and pressure distributions, the Mach discs are clearly distinguished.

The variables needed for the IR-calculation was the temperature, the mass fraction and either the density or the pressure. From the mass fraction, the concentration of species was calculated as partial pressure [1]. The partial pressure was needed to calculate the correct absorption coefficients.

Figure 7. Different distributions from the CFD-solution.



## 4.2 Definition of validation cases

In the experimental-measuring position  $M_1$ , most of the signature will originate from the plume, while for measuring position  $M_2$  both the plume and hot parts of the engine rig contribute to the signature. Since walls were not taken into consideration in this validation, only a comparison with data from measuring position  $M_1$ , i.e. a measuring angle of  $90^\circ$ , was done.

All calculations were done in a wave-number interval from  $1500\text{ cm}^{-1}$  to  $4500\text{ cm}^{-1}$ . Three different resolutions were chosen,  $5\text{ cm}^{-1}$ ,  $16\text{ cm}^{-1}$  and  $25\text{ cm}^{-1}$ . The two first resolutions corresponded to the resolutions used in the experiment while the last resolution was chosen due to special interest in theoretical comparisons.

The angular resolution for each pixel was  $0.1^\circ$  in both  $\theta$ - and  $\phi$ -direction, i.e.  $\Delta\theta = \Delta\phi = 0.1^\circ$ . The  $\theta$ -direction was defined to run along the x-axis and the  $\phi$ -direction in y-direction, see Figure 5. The number of pixels used were  $20 \times 20$ , giving a field-of-view of  $2^\circ$  in  $\theta$  and  $\phi$ , or  $20 \times 10$ , giving a field-of-view of  $2^\circ$  in  $\theta$  and  $1^\circ$  in  $\phi$ .

The species considered in the calculations were  $\text{CO}_2$  and  $\text{H}_2\text{O}$ . The data base of absorption coefficients for these species was extracted from HITRAN and HITEMP [7, 8]. One data base for each wave-number resolution was generated. Means of emission lines were calculated, using the line strengths and Lorentz broadening [7, 9] given by HITRAN and HITEMP.

### Case no. 1

In the first case, the effect of moving the imaginary sensor, section 2, along the x-axis was examined. Both the view position and target position were varied to maintain an angle of  $90^\circ$  to the engine rig. Different parts of the plume were seen, for case no. 1a only half the plume was expected to be seen and for case no. 1c most part of the plume was expected to be seen. Case no. 1c is the case, which corresponds geometrically to the experiment.

### Case no. 2 and no. 3

As discussed above, calculations for different wave-number resolutions needed to be done. In case no. 2 and 3, spectra with resolution  $16\text{ cm}^{-1}$  and  $25\text{ cm}^{-1}$  were calculated, using the view position that covers most of the plume (corresponding to case no. 1c). These calculations were to be compared to each other, case no. 1c and experimental data.

### Case no. 4

The engine test rig is axisymmetric in space, section 4.1. This means that it should not matter from which direction the object is seen as long as the x-coordinate is constant, see Figure 6. It is important to test this, since in many cases, such as this validation case, the CFD-solution is only represented in one quadrant due to the axisymmetry. In case no. 4, this was tested by choosing three different view positions, which were constant in x but that vary in y and z, while the target position is held constant. Rays were drawn both through the real and the virtual part of the mesh.

Case no. 5

The result of the calculation done by SIGGE is very dependent on the CFD-solution. This is very hard to test, but one simple test is to change the temperature. In case no. 5, the temperature was changed by 10% both up- and downwards.

For a better overview, the different cases are summarised in Table 1.

Table 1. The validation cases, see also Figure 5.

Case no.	View position	Target position	Total field-of-view [no. of pixels]		Total field-of-view [degrees]		Directions of Detector Array		Wave number [cm <sup>-1</sup> ]	Angle	
			$\theta$	$\phi$	$\theta$	$\phi$	$\hat{\theta}$	$\hat{\phi}$			interval
1a	(0, 0, L <sub>1</sub> )	(0, 0, 0)	20	20	2	2	(1,0,0)	(0,1,0)	1500-4500	5	90°
1b	(0.008·L <sub>1</sub> , 0, L <sub>1</sub> )	(0.008·L <sub>1</sub> , 0, 0)	20	20	2	2	(1,0,0)	(0,1,0)	1500-4500	5	90°
1c	(0.015·L <sub>1</sub> , 0, L <sub>1</sub> )	(0.015·L <sub>1</sub> , 0, 0)	20	20	2	2	(1,0,0)	(0,1,0)	1500-4500	5	90°
1d	(0.023·L <sub>1</sub> , 0, L <sub>1</sub> )	(0.023·L <sub>1</sub> , 0, 0)	20	20	2	2	(1,0,0)	(0,1,0)	1500-4500	5	90°
2	(0.015·L <sub>1</sub> , 0, L <sub>1</sub> )	(0.015·L <sub>1</sub> , 0, 0)	20	20	2	2	(1,0,0)	(0,1,0)	1500-4500	16	90°
3	(0.015·L <sub>1</sub> , 0, L <sub>1</sub> )	(0.015·L <sub>1</sub> , 0, 0)	20	20	2	2	(1,0,0)	(0,1,0)	1500-4500	25	90°
4a	(0.015·L <sub>1</sub> , 0, L <sub>1</sub> )	(0.015·L <sub>1</sub> , 0, 0)	20	10	2	1	(1,0,0)	(0,1,0)	1500-4500	5	90°
4b	(0.015·L <sub>1</sub> , L <sub>1</sub> , 0)	(0.015·L <sub>1</sub> , 0, 0)	20	10	2	1	(1,0,0)	(0,0,1)	1500-4500	5	90°
4c	(0.015·L <sub>1</sub> , -c <sub>45</sub> ·L <sub>1</sub> , -c <sub>45</sub> ·L <sub>1</sub> )	(0.015·L <sub>1</sub> , 0, 0)	20	10	2	1	(1,0,0)	(0,-1,1)	1500-4500	5	90°
5a <sup>1</sup>	(0.015·L <sub>1</sub> , 0, L <sub>1</sub> )	(0.015·L <sub>1</sub> , 0, 0)	20	20	2	2	(1,0,0)	(0,1,0)	1500-4500	5	90°
5b <sup>2</sup>	(0.015·L <sub>1</sub> , 0, L <sub>1</sub> )	(0.015·L <sub>1</sub> , 0, 0)	20	20	2	2	(1,0,0)	(0,1,0)	1500-4500	5	90°

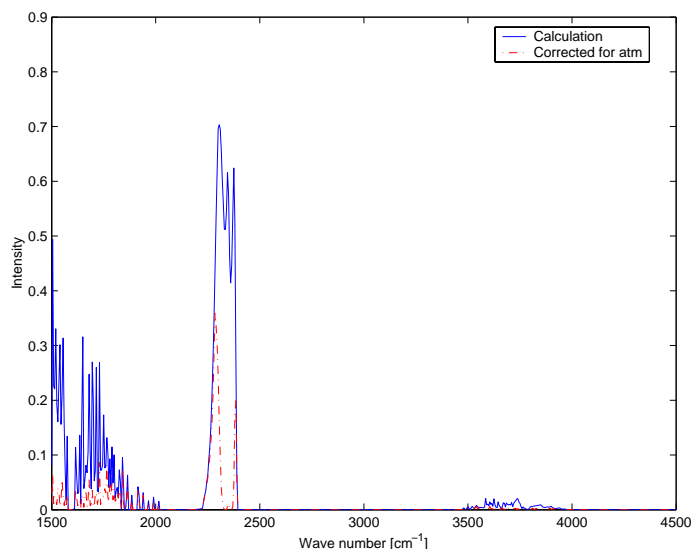
c<sub>45</sub> = cos(45°)<sup>1</sup>Temperature = 110% of original temperature<sup>2</sup>Temperature = 90% of original temperature



## 5 Results

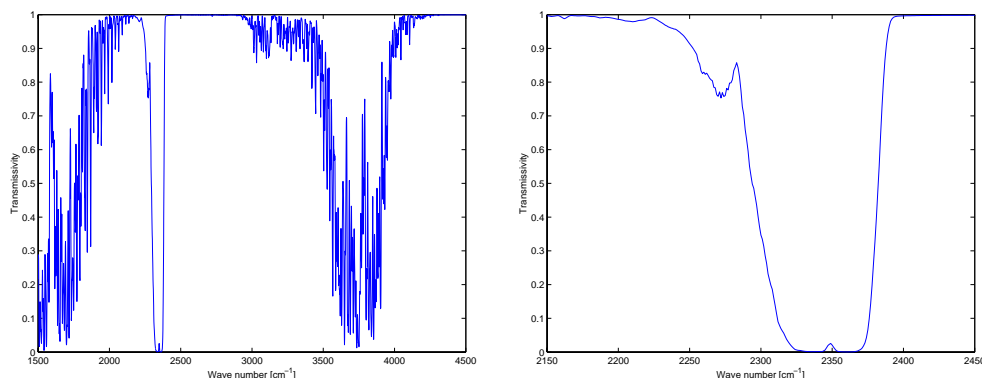
In the resulting spectra, all pixels are added together and, due to reason of publishing, the spectral intensity is normalised to one. An example for case no. 1c is presented in Figure 8. The calculated spectra had to be corrected for the at-

Figure 8. Example of spectrum from case no. 1c together with corresponding spectrum corrected for the transmissivity in the atmosphere.



mospheric moderation, see section 2. Thus, the spectra were multiplied with the transmissivity in the atmosphere, Figure 9, giving an approximate correction. The transmissivity was generated by MODTRAN [10], assuming a distance to target of 20 m, an air humidity of 35%, an air temperature of 290 K and the air type subarctic summer.

Figure 9. Transmissivity in the atmosphere, calculated by MODTRAN for the validation case.



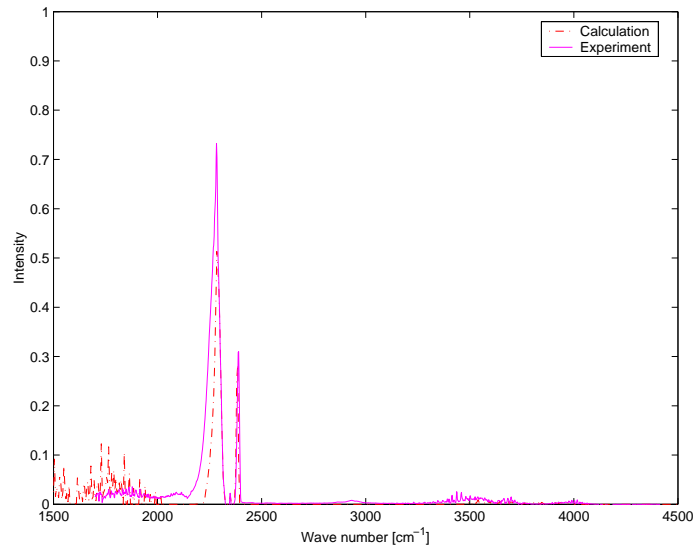
(a) The whole wave number interval.

(b) Enlarged wave number interval.

The corrected spectra were compared with experimental data from the measurement described in section 3, see example in Figure 10. Different peaks in the

spectrum correspond to different species. The peaks up to  $\sim 2000 \text{ cm}^{-1}$  and the peaks in the interval  $3500 \text{ cm}^{-1} - 4000 \text{ cm}^{-1}$  correspond to  $\text{H}_2\text{O}$ . The dominating peaks between  $2200 \text{ cm}^{-1}$  and  $2400 \text{ cm}^{-1}$  correspond to  $\text{CO}_2$ . As seen in Figure

Figure 10. Case no. 1c compared with experimental data.



10, the peaks of  $\text{CO}_2$  were well reproduced, while the peaks of  $\text{H}_2\text{O}$  were not as well estimated. This could be due to the approximations used in the calculations and also due to variations in the air humidity.

### Case no. 1

In this case, spectra from the different view positions were compared with each other and with the experimental data. To be able to make a fair comparison, only a restricted wave-number interval was used,  $\eta = 2100 \text{ cm}^{-1} - 2500 \text{ cm}^{-1}$ , Figure 11.

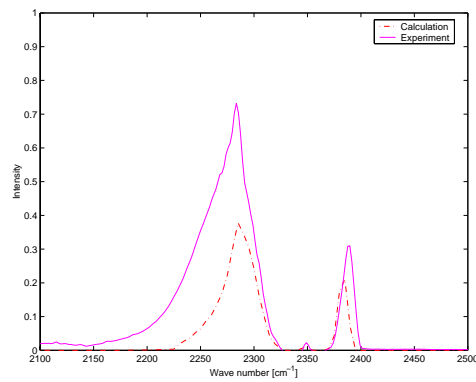
An image of the intensity can also be presented by plotting the integrated intensity value of each pixel. In Figure 12, images from the different view positions are shown. In each pixel, the spectral intensity was integrated over the interval  $1500 \text{ cm}^{-1} - 4500 \text{ cm}^{-1}$ . The angular resolution is  $\Delta\theta = \Delta\phi = 0.1^\circ$ .

As seen in Figure 11, case no. 1c gives the best agreement to the experiment as this case covers most of the plume, Figure 12. This is the expected result.

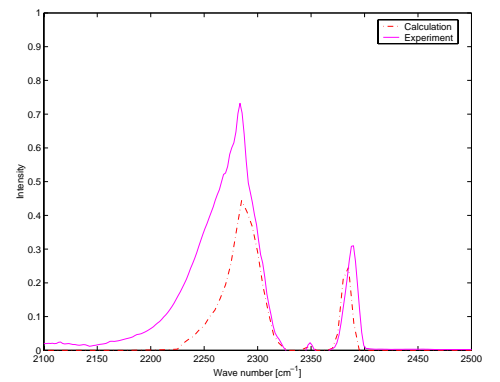
In Figure 13, an image of the best case (1c) is presented with higher angular resolution,  $\Delta\theta = 0.02^\circ$  and  $\Delta\phi = 0.05^\circ$ . Here, the Mach discs are clearly seen.



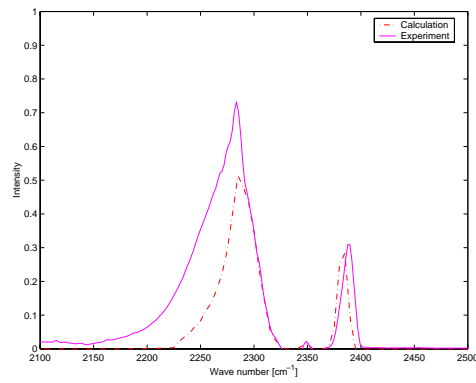
Figure 11. Spectra for the different view positions in case no. 1.



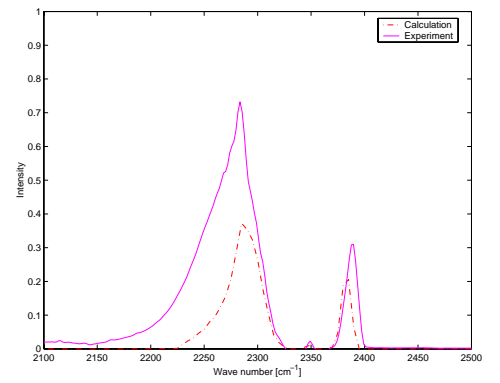
(a)  $x = 0$



(b)  $x = 0.008 \cdot L_1$



(c)  $x = 0.015 \cdot L_1$



(d)  $x = 0.023 \cdot L_1$

Figure 12. Images for the different view positions in case no. 1. The colour scale is the same in all pictures.

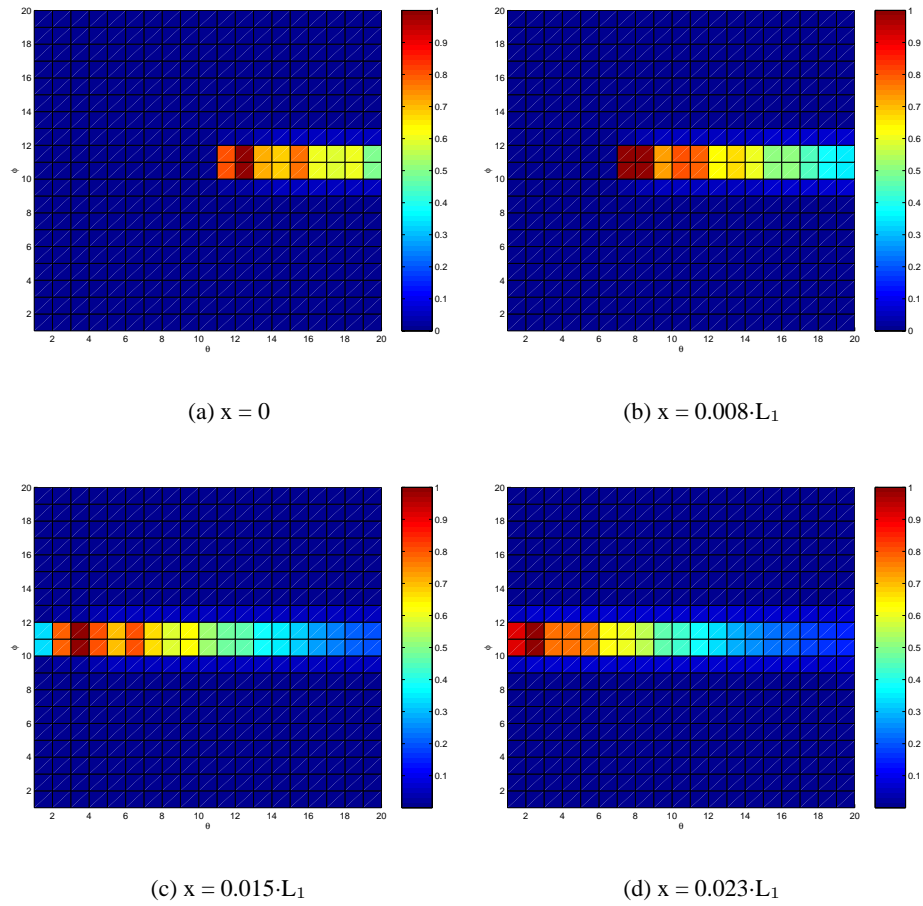
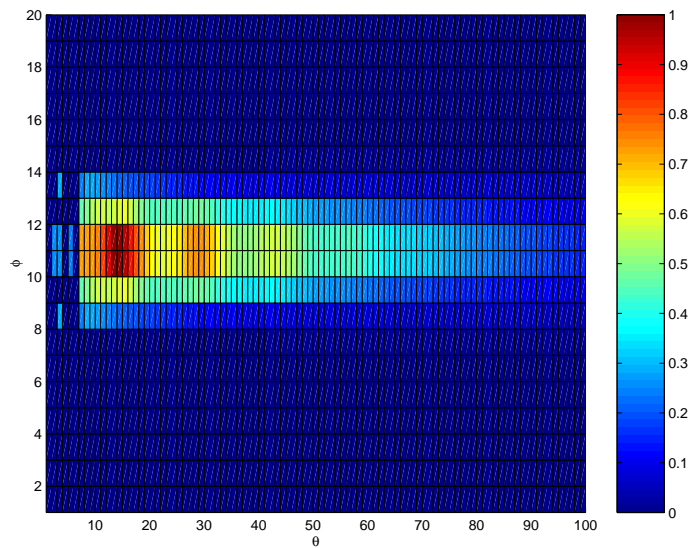


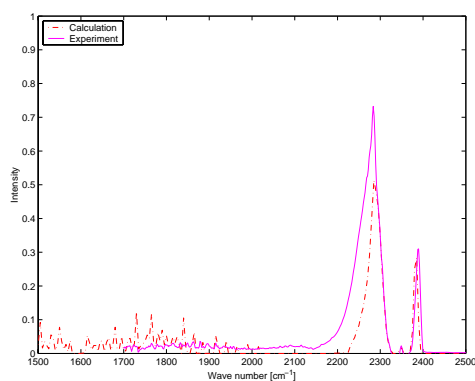
Figure 13. High angular resolution image,  $\Delta\theta = 0.02^\circ$  and  $\Delta\phi = 0.05^\circ$ , corresponding to case no. 1c.



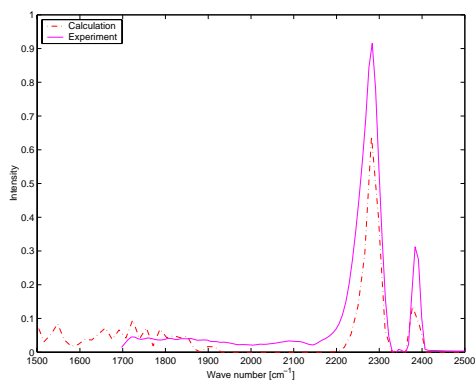
### Case no. 2 and 3

In Figure 14, spectra with resolution  $5\text{ cm}^{-1}$ ,  $16\text{ cm}^{-1}$  and  $25\text{ cm}^{-1}$  are shown. The calculations were made in a view position corresponding to  $x = 0.015 \cdot L_1$ . The calculated spectra are compared with experimental data of resolution  $\Delta\eta = 4\text{ cm}^{-1}$  in Figure 14(a) and data of resolution  $\Delta\eta = 16\text{ cm}^{-1}$  in Figure 14(b) and (c).

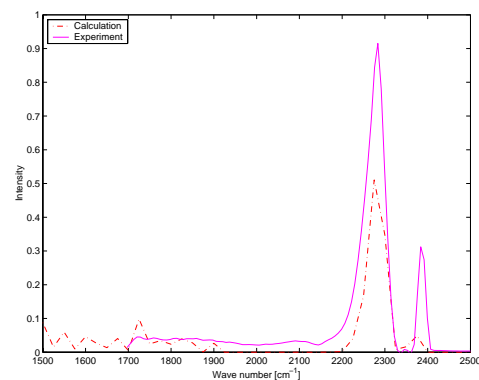
Figure 14. Comparison of spectra with different resolutions.



(a)  $\Delta\eta = 5\text{ cm}^{-1}$  (calculation) and  $\Delta\eta = 4\text{ cm}^{-1}$  (experiment)



(b)  $\Delta\eta = 16\text{ cm}^{-1}$



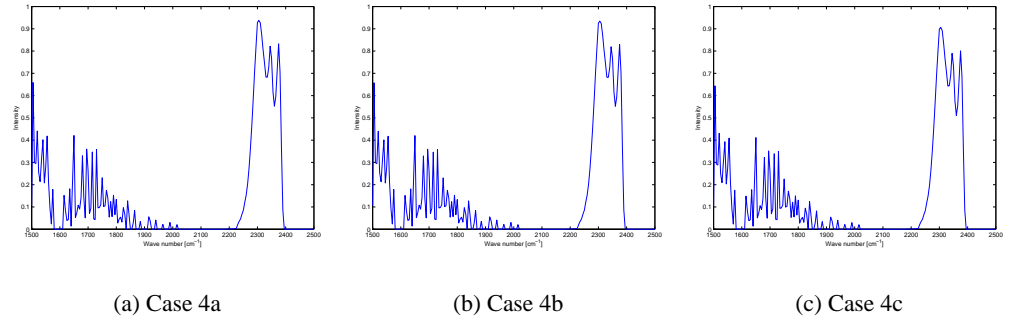
(c)  $\Delta\eta = 25\text{ cm}^{-1}$  (calculation) and  $\Delta\eta = 16\text{ cm}^{-1}$  (experiment)

It is seen that calculations made with different resolution gave similar result. In comparison with the experimental data for the CO<sub>2</sub>-peaks, the highest resolution,  $\Delta\eta = 5\text{ cm}^{-1}$ , gave the best agreement. Resolutions  $\Delta\eta = 16\text{ cm}^{-1}$  and  $\Delta\eta = 25\text{ cm}^{-1}$  gave acceptable agreements, but it should be remembered that the experimental data corresponds to a resolution of  $16\text{ cm}^{-1}$ . As seen in previous calculation, the H<sub>2</sub>O-peaks were not as well reproduced.

**Case no. 4**

In Figure 15, spectra with different but axisymmetrical view positions are presented. These spectra were not corrected for transmissivity in the atmosphere, since they should just be compared to each other and not to experimental data.

Figure 15. Spectra for the different view positions in case no. 4.

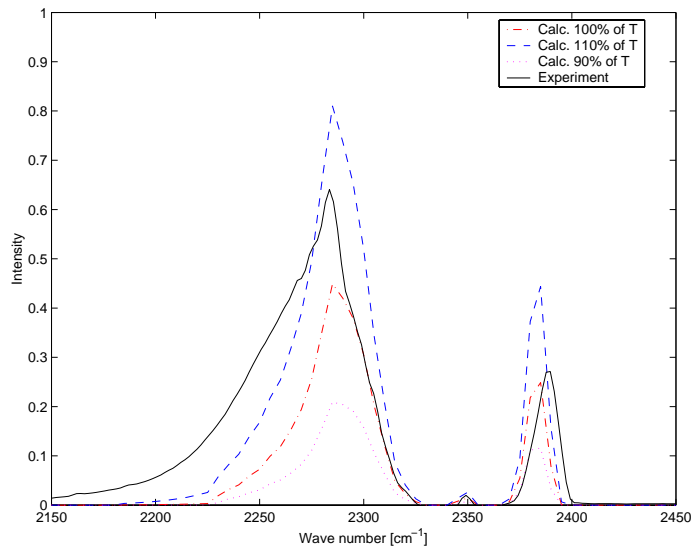


Due to the axisymmetrical character of the problem, these spectra should be identical, which is the case.

**Case no. 5**

In Figure 16, the impact of changes of the temperature in the CFD-solution is shown. It is clearly seen that the quality of the CFD-solution will effect the result of the IR-calculation.

Figure 16. Comparing the impact of changing the temperature in the CFD-solution.



## 6 Conclusions and outlook

Two modules of the module base program SIGGE has been validated for IR-calculations of a hot gas. The objects that have been validated are:

1. *The impact of moving the view position in one direction while keeping the angle to the target constant. The result was compared with experimental data.*
2. *How the result will depend on the resolution. The result of the different resolutions,  $\Delta\eta = 5 \text{ cm}^{-1}$ ,  $16 \text{ cm}^{-1}$  and  $25 \text{ cm}^{-1}$ , were both compared to each other and to experimental data.*
3. *The ability to use axisymmetrical CFD-solution.*
4. *The impact of the quality of the CFD-solution. The temperature was shifted up and down by 10%.*

Taking into account the error sources: The absorption coefficient data base, the calculation of distribution of species [1], the simple model used etc, all above items were sufficiently satisfied:

1. *The calculation of the view position, which was expected to give the best agreement with the experimental result, actually reproduced the experiment best.*
2. *The different resolutions gave similar result and they reproduced the corresponding experimental data well.*
3. *Spectra from different axisymmetrical view positions gave identical spectra.*
4. *The impact of the changes of the temperature was clearly seen. Thus, the choice of CFD-solution has to be done carefully.*

The conclusion is that the code itself works as expected. Experimental data is reproduced satisfactory. Thus, it is strongly justified that the development of SIGGE will continue.

The absorption coefficients can be extracted in several ways, for example by considering line-by-line absorption coefficients or by statistic band models. In this validation case, a mean of the emission lines has been used. Ways of extracting absorption coefficients will be investigated in the future.

Considering the error sources discussed above, it is seen that only one of them is directly a part of SIGGE itself, namely, the simple model used, i.e no specific models for the different species. This is something that will be worked on in the future. Also the capability of handle walls in a correct way will be added as well as handling atmospheric background and transmission. This will be accompanied with further validations.

In the present  $\beta$ -version of SIGGE, only the spectral intensity is calculated. In the next version, radiance calculations will be implemented.



## Acknowledgements

The Department of IR Systems, Sensor Technology, FOI, is acknowledged for sharing their experimental data and knowledge in the IR-field.

The Department of Military Engines, at Volvo Aero Corporation in Trollhättan, is acknowledged for contributing with the CFD-data and for sharing their expertise.





## References

- [1] M. Andersson , *Derivation of the Equations used by the Computer Program SIGGE for Calculating IR-intensity*, FOI-R-0553-SE, (2002).
- [2] M. Andersson et. al., *SIGGE VI.0 $\beta$ , Users Guide*, FOI-R-0554-SE, (2002).
- [3] P. Nilsson and C. Nelsson, *Spectral IR-measurement on an engine test rig - Trollhättan 2000*, FOI-RH-0067-SE, (2001).
- [4] F. Lundberg, *The design of ScanSpec - a scanning imaging FTIR spectrometer*, FOA-R-99-01041-615-SE, (1999).
- [5] C. Nelsson et. al., *ScanSpec, an imaging spectrometer*, SPIE 4029, (2000).
- [6] L.E. Eriksson, *A Third Order Accurate Upwind-Biased Finite-Volume Scheme for Unsteady Compressible Viscous Flow*, Technical report, VAC Report 9370-154, Volvo Aero Corporation, Sweden (1990).
- [7] L.S. Rothman et. al., *The HITRAN Molecular Spectroscopic Database and HAWKS (HITRAN Atmospheric Workstation): 1996 Edition*, Journal of Quantitative Spectroscopy and Radiative Transfer, vol. **60**, pp. 665-710, (1998).
- [8] *The HITRAN Database*, <http://www.hitran.com>.
- [9] M.F. Modest, *Radiative Heat Transfer*, McGraw Hill, pp. 334, (1993).
- [10] *MODTRAN*, <http://www.ontar.com>.



Issuing organisation FOI – Swedish Defence Research Agency Division of Aeronautics, FFA SE-172 90 STOCKHOLM	Report number, ISRN FOI-R-0555-SE	Report type Technical report
	Month year August 2002	Project number E840346
	Customers code 3. Aeronautical Research	
	Research area code 7. Vehicles	
	Sub area code 73. Aeronautical Research	
Author(s) Marlene Andersson	Project manager Marlene Andersson	
	Approved by Bengt Winzell Head, Computational Aerodynamics Department	
	Scientifically and technically responsible Marlene Andersson	
Report title Validation of the Computer Program SIGGE against Spectral IR-measurements on an Engine Test Rig		
Abstract The IR-signature code SIGGE has been validated, using spectral IR-measurements on an engine test rig. Calculations of IR-radiation from gases, such as CO <sub>2</sub> and H <sub>2</sub> O, have been compared with experimental data. The calculations have been made in the wave-number interval $\eta = 1500 \text{ cm}^{-1} - 4500 \text{ cm}^{-1}$ , with three different resolutions, $\Delta\eta = 5 \text{ cm}^{-1}$ , $16 \text{ cm}^{-1}$ and $25 \text{ cm}^{-1}$ . The result is satisfactory and further developments of SIGGE will proceed.		
Keywords IR-signature, SIGGE, validation, plume, flame		
Further bibliographic information		
ISSN 1650-1942	Pages 35	Language English
	Price Acc. to price list	
	Security classification Unclassified	



Utgivare Totalförsvarets Forskningsinstitut – FOI Avdelningen för Flygteknik, FFA SE-172 90 STOCKHOLM	Rapportnummer, ISRN FOI-R-0555-SE	Klassificering Teknisk rapport
	Månad år Augusti 2002	Projektnummer E840346
	Verksamhetsgren 3. Flygteknisk forskning	
	Forskningsområde 7. Bemannade och obemannade farkoster	
	Delområde 73. Flygteknisk forskning	
Författare Marlene Andersson	Projektledare Marlene Andersson	
	Godkänd av Bengt Winzell Chef, Institutionen för beräkningsaerodynamik	
	Tekniskt och/eller vetenskapligt ansvarig Marlene Andersson	
Rapporttitel Validering av Datorprogrammet SIGGE mot Spektrala IR-mätningar utförda på en Motortestrigg		
Sammanfattning IR-signaturkoden SIGGE har blivit validerad med hjälp av spektrala IR-mätningar utförda på en motortestrigg. Beräkningar av IR-strålning från gaser, som CO <sub>2</sub> och H <sub>2</sub> O, har jämförts med experimentella data. Beräkningarna har gjorts i vågtalsintervallet $\eta = 1500 \text{ cm}^{-1} - 4500 \text{ cm}^{-1}$ , med tre olika upplösningar, $\Delta\eta = 5 \text{ cm}^{-1}$ , $16 \text{ cm}^{-1}$ och $25 \text{ cm}^{-1}$ . Resultatet är tillfredställande och utvecklingen av SIGGE kommer att fortgå.		
Nyckelord IR-signatur, SIGGE, validering, plym, flamma		
Övriga bibliografiska uppgifter		
ISSN 1650-1942	Antal sidor 35	Språk Engelska
Distribution enligt missiv	Pris Enligt prislista	
	Sekretess Ej hemlig	